ROBERT C. BEAL

PREDICTING DANGEROUS OCEAN WAVES WITH SPACEBORNE SYNTHETIC APERTURE RADAR

High waves have always been a major menace to marine activities. They can unexpectedly overwhelm ships, gradually stress and occasionally uproot off-shore towers, and erode and destroy beaches and coastal structures. Spaceborne synthetic aperture radar may one day enhance our ability to predict these dangerous waves anywhere on the globe.

INTRODUCTION

Few of us have ever experienced the raw force of a truly extreme storm wave. Under the action of a persistently strong wind, ocean waves can grow into giant mountains of water that threaten even the largest ships. The highest credibly recorded storm wave measured 34 meters from crest to trough.[1] No doubt even higher waves occur, but they are unlikely to be recorded in situ. Winter storm waves in the North Atlantic, in the Gulf of Alaska, and in the Southern Oceans between 40° and 60°S latitude often exceed 10 meters, and, when these waves run adversely into a strong current, they can be amplified by a factor of two. Resulting "rogue" waves are regularly reported just off the southeast coast of South Africa where they are notorious for their hazard to ships attempting to take advantage of the southwesterly flowing Agulhas Current.

The state of the sea has always played a major role in human affairs. Students of history will recall a number of pivotal naval encounters, the results of which were strongly influenced by sea state. One of the more well known occurred in 1588, when the fragmented Spanish Armada, under pursuit by the highly maneuverable English fleet, attempted retreat by way of the North Sea.[2] Ravished by strong gales for nearly two weeks, the invincible Armada was demoralized and demolished. Spanish naval power and influence never recovered.

More recently, U.S. Navy Captain C.R. Calhoun recounts[3] a tragedy experienced by the Third Fleet in the Pacific typhoon of December 1944. Incorrect forecasting, poor ship design, and lack of communication combined to decimate much of that fleet in a single storm. Three destroyers, more than 100 carrier aircraft, and 778 lives were lost. Figure 1 shows damage inflicted by the storm on a surviving carrier, the USS *Bennington*, all of whose aircraft were destroyed in the hangar.

Catastrophes such as these, which consume more lives and property than most naval battles, form a major incentive for research toward the understanding of ocean waves. Today, more than a hundred ships a year are overwhelmed by the sea, according to Lloyd's of London, the international marine insurance agency. Even this is a much better record than a century ago, when thousands of wooden ships were lost to storms every year.[4]

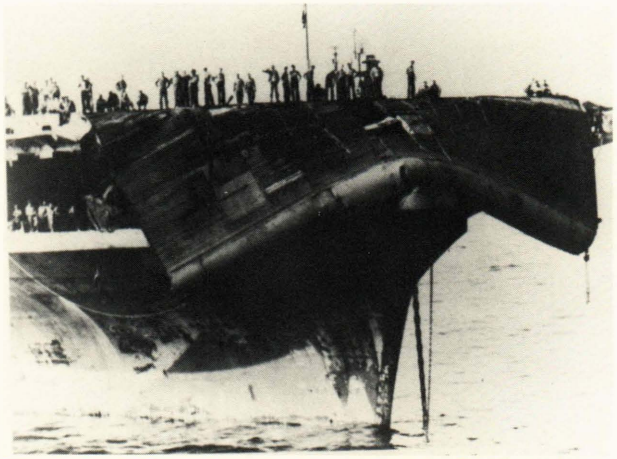

Figure 1—USS *Bennington*, damaged by the Pacific typhoon of December 1944.

THE GENERATION OF WAVES BY WIND

Wind and waves have been known since antiquity to be coupled. It seems only reasonable, then, to expect that a complete knowledge of the wind field might lead to a complete knowledge of the wave field. The wind-wave relationship is complicated, however, because the air-sea boundary (i.e., the wave field) is not only moving in time and space, but is continually influencing and modifying the very wind that causes the waves. Furthermore, the wind energy is converted not only into waves, but also into a surface drift current and a turbulent mixing of the upper layer of the ocean. This partitioning of energy is a highly nonlinear and interdependent process, especially in the extreme conditions that are of most interest.

As early as 1871, Lord Kelvin applied the results of Helmholtz's study of fluids to a two-layer (air-sea) problem. For a critical value of differential velocity (approximately 6.5 meters per second) (m/sec), he found that small disturbances at the boundary became unstable, producing monotonic growth. In 1924, Jeffries[5] attacked the problem of more realistic propagating waves and introduced the notion of a "sheltering coefficient." When the wind velocity exceeds the phase velocity of the wave, energy is transferred from wind to wave, resulting in wave growth. Equilibrium is established when the two are about equal. This result is, in fact, quite close to reality. However, Jeffries idealized the ocean surface as a simple sinusoid, and he failed to recognize the importance of surface drag. In 1956, Ursell[6] suggested that future model development should incorporate turbulent air streams with random (statistically stationary) stresses. Here was one of the first clear statements of the fundamentally nondeterministic nature of ocean waves.

Meanwhile, during World War II, operational wave forecasting had become a critical problem. Pierson, Neumann, and James[7] were the first to incorporate statistical concepts into a wave forecast model. The concept of an "ocean wave spectrum" was introduced, with the wind acting independently on each Fourier component and the individual component amplitudes empirically determined by the duration and fetch (i.e., time and distance over which the wind acts). These early operational models were entirely empirical, but they strengthened the concept of the ocean as a random, temporally and spatially varying, surface whose only significant descriptors were statistical. The ocean wave energy spectrum became recognized as perhaps the single most significant descriptor of the ocean surface.

The generation, propagation, and dissipation of the spectrum under arbitrary conditions continue to be controversial, even after 30 years of research and debate. Much of the controversy persists simply because there is no good way to monitor accurately the ocean spectrum, particularly in extreme conditions.

THE FULL TWO-DIMENSIONAL (DIRECTIONAL) SPECTRUM

In much of the above discussion and, indeed, in much of the early theoretical development of the concept, the ocean spectrum is implicitly assumed to be virtually unidirectional; that is, the ocean waves are assumed to travel principally in the direction of the local wind. This is, of course, an extremely simplistic assumption and of only limited practical use. In reality, there exists a fairly complicated directional distribution of wave energy composed, for example, of "swell" from a remote generation area and "sea" from the local wind. Moreover, each of the wave systems exhibits distinct directional properties, and each experiences a separate and distinct evolution of its dominant wavelength and direction over both time and space. A thorough understanding of this evolving directional spectrum is the key to accurate wave forecasting.

The importance of direction is not difficult to appreciate if we consider the nature of the forces that work to capsize or impede a ship on a stormy sea. All buoyant objects have a natural period (or frequency) of oscillation. Oceangoing vessels are designed to be fast and fuel-efficient, yet stable. Often, however, stability is sacrificed for speed and efficiency, the result being a higher ship responsivity to external driving forces.

Typically, a ship's response to wave forcing is extremely directionally sensitive. And yet, in a storm where "crossed" (multidirectional) seas are the rule rather than the exception, the proper heading and speed of a vessel cannot be determined easily by pilot intuition. Similar trade-offs must be made in the design of off-shore towers. These towers are the largest structures ever built by man and are extremely expensive to construct and deploy,[8] yet they need not be equally resistant to wave forcing from all directions. A good knowledge of local directional wave climatology could result in more efficient and less expensive tower designs.

Traditionally, accurate measurements of the directional spectrum have been extremely difficult to make. Stereophotography from aircraft was attempted in the 1950s, but timing and spatial registration problems severely limited the accuracy of the results. In the 1960s, directional buoys were developed by the British, but their directional resolution is limited, and their expense and maintenance requirements make them impractical for routine measurements over large areas of the ocean.

THE POTENTIAL OF SYNTHETIC APERTURE RADAR

Synthetic aperture radar (SAR), although conceived in principle in the early 1950s, became practical only through the ingenious application of large- aperture, high-quality optics in the early 1960s. Nearly simultaneously, at a Woods Hole Conference,[9] a few oceanographers and radio scientists made a strong case for a complement of radar instruments (including an imaging radar) orbiting at an altitude of 700 km. From the preface of the Conference Record:

> Wind waves and swell constitute another field which requires the extended perspective of an elevated viewpoint for complete observation. Attempts to derive the wave field from data taken at a few discrete points are always hopelessly incomplete. What is needed is the directional energy spectrum of waves on a two-dimensional surface, and for this, the vantage point offered by a satellite is ideal. It is within the capability of present day radar technology to give a complete description of the sea surface.

In 1972, the first proposals for Seasat, a dedicated microwave oceanographic satellite, were presented to the U.S. Congress. The measurement of the directional energy spectrum was high on the list of user priori-

ties, although the SAR, because of potential cost, complexity, and lack of scientific verification, had not yet been formally approved for the mission. However, three years later, after extensive aircraft experiments at the Jet Propulsion Laboratory, the National Aeronautics and Space Administration (NASA) committed the SAR to the Seasat mission as an "experimental" instrument, thereby acknowledging its lack of maturity with respect to the other active radar instruments, the altimeter and scatterometer. The promise of SAR was that it might allow the measurement of the directional wave spectrum on global scales, quasi-continuously, and under extreme and variable ocean conditions.

Seasat was launched in June 1978 into a nearly polar orbit at an altitude of 800 km and immediately began collecting ocean data on the global distribution of wind, waves, and currents. The quality and extent of coverage were unprecedented and will likely remain so for nearly the remainder of this decade. Because of a sudden power failure, the Seasat mission lasted for only 100 days; thus many of the longer term experiments were not completed. Even in that short span of time, however, the data set collected by the SAR was so overwhelming that, even now, only a small fraction has been thoroughly analyzed, much of it at APL. Fortunately, however, we are now on the verge of critically assessing the value of SAR for the measurement of directional wave spectra. Not only do we have several years of Seasat analysis behind us, but we are just now beginning to analyze results from the very recent and much better instrumented Shuttle Imaging Radar (SIR-B) ocean-imaging experiment, which occurred from October 5 through 12, 1984.

INFORMATION IN SAR OCEAN IMAGERY

Because the SAR irradiates the ocean surface at about 30 cm wavelength (1.27 gigahertz, modified by the system geometry), any geophysical process that directly or indirectly influences these short 30 cm waves will produce a signature in SAR imagery. The Seasat SAR revealed an unexpectedly rich variety of backscatter patterns from the surface of the ocean.[10,11] Although still far from being fully understood, these patterns occurred on nearly all spatial scales accessible to the SAR, i.e., from its spatial resolution of 25 meters to its full swath width of 100 km. As an example of the kinds of information inherent in SAR imagery, this section describes some of the results from an intensive analysis of a particular Seasat SAR pass spanning about 900 km (pass 1339, September 28, 1978).

Figure 2, derived from an examination of Seasat scatterometer winds over a period of several days, shows the spatial and temporal locations of two separate storm systems as they evolved during the days just prior to pass 1339. Both storms spawned wave systems propagating generally toward the west, i.e., toward the SAR overpass region. The southernmost primary storm was the more intense of the two and reached

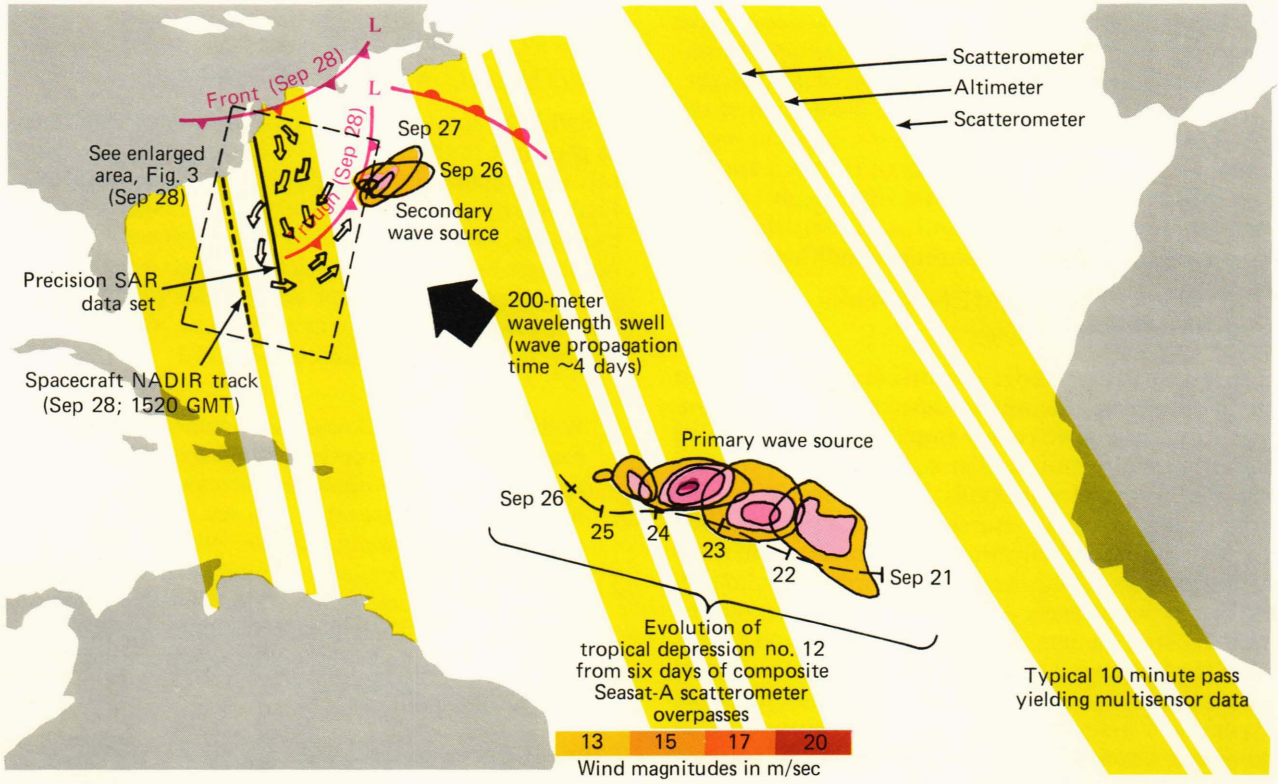

Figure 2—Spatial and temporal locations of two separate storm sources as they evolved during September 1978.

peak winds in excess of 20 m/sec and peak (significant) wave heights of about 6 meters (as measured by the Seasat altimeter) before subsiding. As this wave system approached the east coast of the United States, the average wavelength was about 200 meters, and the wave height had diminished to about 1 meter.

Meanwhile, also from an examination of previous scatterometer wind fields, a somewhat weaker but closer secondary storm had developed about 1000 km from the impending 900-km-long SAR overpass. This wind field reached 15 m/sec and spawned waves that were 2 to 3 meters high. Since the secondary wave source was so much closer to the SAR overpass, however, the SAR-measured wave field experienced rapid spatial evolution.

Figure 3 represents the composite data from a number of different sensors, both satellite and aircraft, including results from the SAR image analysis along the 900 km pass. The analysis of this particular data set at APL has probably been more intensive than any comparable 2 minutes of SAR ocean data in the entire Seasat mission. A number of significant results have emerged in the past 5 years, using (a) high-quality digitally processed SAR data, in combination with auxiliary data from the Seasat scatterometer and altimeter for independent measures of surface wind velocity and wave height; (b) infrared and visible imagery from the Geostationary Satellite (GOES) to track associated storm centers; (c) NASA aircraft estimates of air-sea temperature differences (related to boundary layer stability) and near-surface wind velocity; and (d) isolated buoy and pier measurements of wind and waves at single points. By some measures, the potential of the SAR has exceeded all expectations. On the other hand, fundamental limitations have been exposed, especially in high sea states.

Surface Wind Magnitude

Note on Fig. 3 the sequence of 19 40-km-wide SAR images, spanning the 900 km pass. Although the displayed imagery is not contiguous, it does represent an appreciable fraction of the originally collected 100-km-wide imagery. The average SAR backscatter magnitude is highly correlated with estimates of wind magnitude from the Seasat scatterometer (shown as multidirectional "aliased" vectors on the blue background). As shown in Fig. 4, a power law fit determined by minimizing the spatially averaged residuals yields agreement between the SAR and scatterometer estimates of wind magnitude that is usually better than 1 m/sec all along the 900 km pass. Thus, the SAR (sensing 30-cm surface wave activity) appears to permit as accurate a determination of wind speed as the scatterometer (sensing shorter 3-cm surface wave activity). Moreover, the SAR, with its higher spatial resolution, may contain very fine scale information on the spatial variations of wind speed. Knowledge of these variations might provide new insight into more conventional scatterometer operation, which inherently must average over many tens of kilometers to obtain its estimates of wind speed.

Surface Wind Direction

In nature, there is no such thing as a "uniform" wind field. Even if one could set up such a condition temporarily over the ocean, it would often tend to degenerate into convective "rolls," producing the effect of a spatially varying wind magnitude at the ocean surface with a maximum gradient normal to the dominant wind direction. The rolls are particularly pronounced above about 5 m/sec and when the ocean is warmer than the air. In the early 1940s, Woodcock[12] noted this same effect in the linear soaring patterns of sea gulls as they took advantage of the natural lift on the updraft sides of the rolls.

The characteristic cross dimension of these rolls is several kilometers. Because they can produce a spatial modulation of the wind magnitude at the ocean surface, the Seasat SAR imagery often (perhaps nearly always) contains an identifiable signature of the local wind direction. Occasionally the signature is readily identifiable as streaks in the imagery that are generally aligned with the wind. More often, it is so subtle that only a sophisticated combination of spectral and spatial averaging will identify it. Only the very low spatial frequencies contain the pertinent information; spatial samples of at least a few kilometers are necessary. The associated two-dimensional Fourier transforms exhibit a pronounced radial asymmetry, with a major axis approximately normal to the local wind direction.[13]

Figure 3 contains (in the column labeled "SAR Wind Spectra") a full set of color-coded spectra for the entire pass, spatially averaged over areas of 6 × 32 km, corresponding to the area encompassed by the white squares within each 40 km SAR image. The spectra are displayed linearly in wavenumber (equal to 2π radians per wavelength), with the outer circle corresponding to an 800 meter wavelength. When the direction of the normal to the principal axis is plotted against locally averaged estimates of wind direction from the scatterometer, the curve of Fig. 5 results, demonstrating that, in this case at least, the SAR determinations of local wind direction are at least as accurate as those of the scatterometer. Indeed, there is good reason to believe that the SAR is revealing fine-scale natural fluctuations in the surface wind field that might eventually help to explain variability in the scatterometer wind direction estimates.

Ocean Wave Spectra

As interesting and unexpected as the *wind* signatures might be, the original motivation for the Seasat SAR was to measure the directional *wave* spectra. Fortunately, the ocean wavelengths of interest do not generally overlap the wind row dimensions: wind-generated waves longer than 500 meters or shorter than 50 meters generally contain little energy. These ranges of surface waves are visible in Seasat SAR imagery because their orbital velocity produces a periodic spatial modulation of the local wind-generated 30 cm waves. The modulation may be much less than the noise on the scale of a single 25-meter resolution ele-

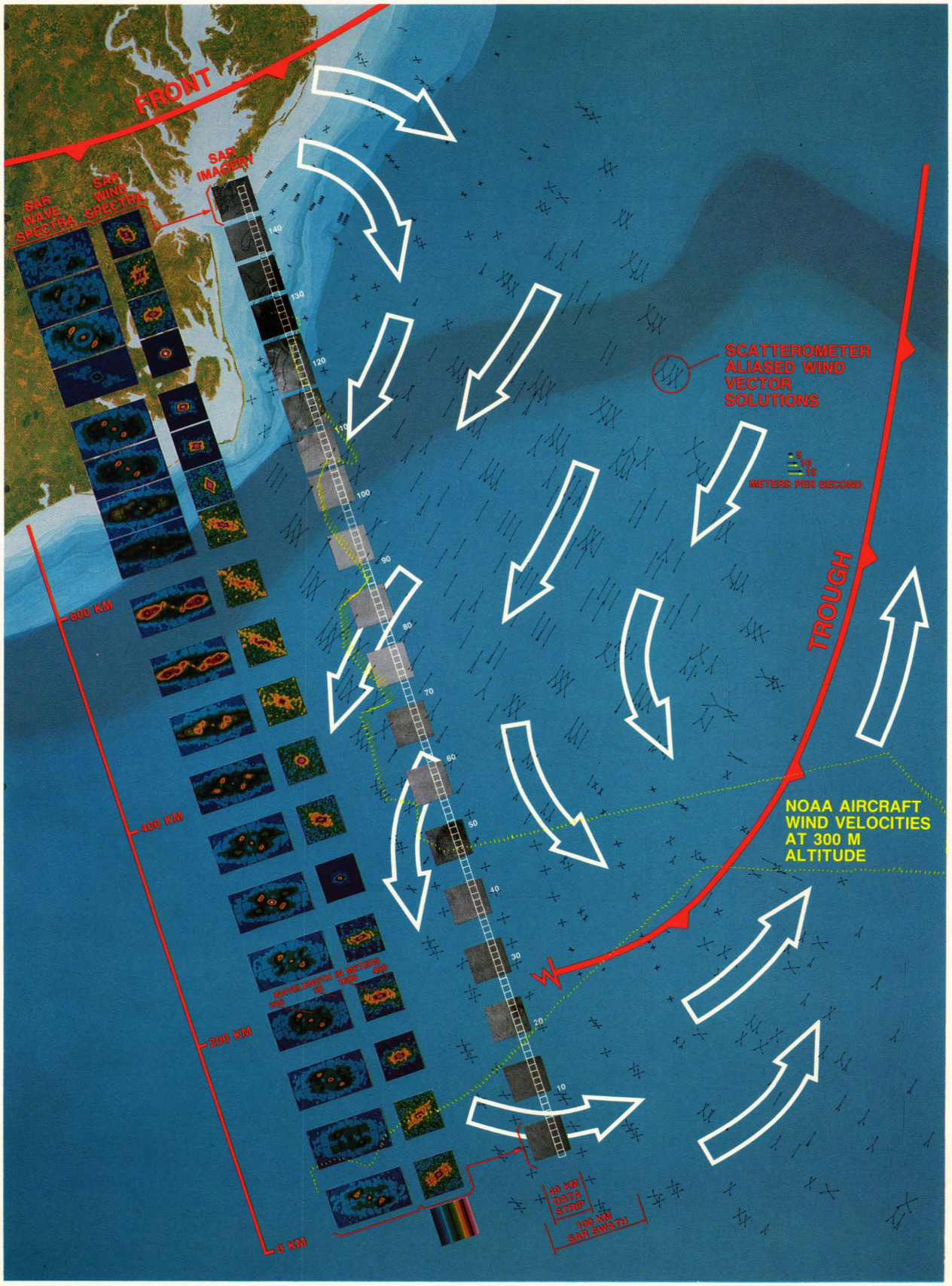

Figure 3—Composite data sources, SAR imagery, and corresponding wind and wave spectra for Seasat SAR pass 1339, September 28, 1978.The straight red line shows the satellite nadir track (ascending pass).

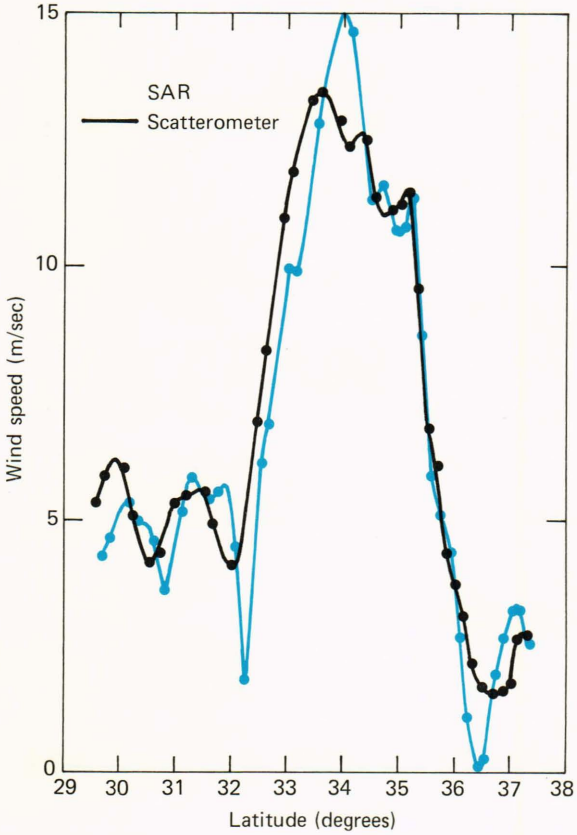

Figure 4—Comparison of wind magnitude estimates from both the scatterometer and the SAR.

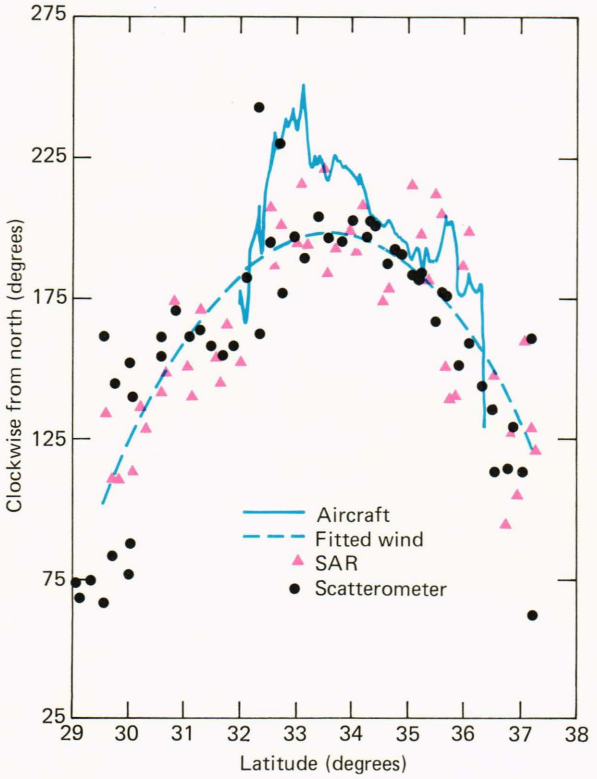

Figure 5—Comparison of wind direction estimates from both the scatterometer and the SAR.

ment, but the spatial spectrum of the wave field, at least in deep water, is generally well-behaved and homogeneous over several tens of kilometers. Extensive averaging over both wavenumber and space, therefore, can reduce a very noisy background by as much as a factor of 20 or 30, revealing extremely subtle modulations of only a few percent.

Figure 3 (in the column labeled "SAR Wave Spectra") shows a full set of spatially evolving wind-wave spectra along the entire 900 km pass. All the spectra are radially symmetric with 180° ambiguity in the direction of wave propagation. The spectra are again displayed linearly in wavenumber, with the outer circle corresponding to a 50 meter wavelength. The spectra change quite rapidly in the center region of the pass, where a locally strong wind has produced a dominant (70 meter wavelength) tertiary wave system over the middle 100 km or so.

Figure 6 shows in greater detail how some of the more subtle modulations can be emphasized with a proper combination of spectral and spatial averaging. Figures 6a and 6b are replicas of the first (moderate wind-wave) and tenth (high wind-wave) SAR images from the bottom, respectively, in Fig. 3. Each has been corrected for a cross-swath intensity falloff; precorrected image samples with their associated trends are shown in the green-bordered imagery. In Fig. 6a, an area just below the trough of Fig. 3, the surface wind is 3 to 5 m/sec from the northwest; in Fig. 6b, the surface wind is 10 to 12 m/sec from the northeast. Figure 6c contains a set of highly magnified 3 × 6 km regions from each 40 km image and illustrates a dramatic change in the texture of the imagery as the wind increases. The moderate wind sample is taken from frame 3 on Fig. 3; the high wind sample is from frame 85.

Figures 6d and 6e are each composites of wave spectra taken from the respective moderate and high wind images of Figs. 6a and 6b. The format is similar to that of the Fig. 3 wave spectra, with the outer circle corresponding to an ocean wavelength of 50 meters. To illustrate the effect of spatial averaging, the left halves of the spectra are derived from a single 6-km-square area (frames 3 and 85 in Fig. 3), while the right halves are averages of six sequential spectra (frames 1 to 6 and 81 to 86 in Fig. 3). Although the averaged spectra contain lower noise, they obscure spectral variations on local scales. Note that there has been a substantial evolution of the ocean waves along the 500 km separating the spectra of Figs. 6d and 6e. The two shorter wavelength (longer wavenumber) systems dominating the high wind spectra are entirely absent in the more southerly spectrum.

The very center (low wavenumber) region of the spectrum contains information on surface wind speed and direction, as discussed in the above section. Subtleties in low wavenumbers (corresponding to surface wavelengths of several kilometers) cannot always be extracted with 6 km image samples. For example, the central square regions in the centers of Figs. 6d and

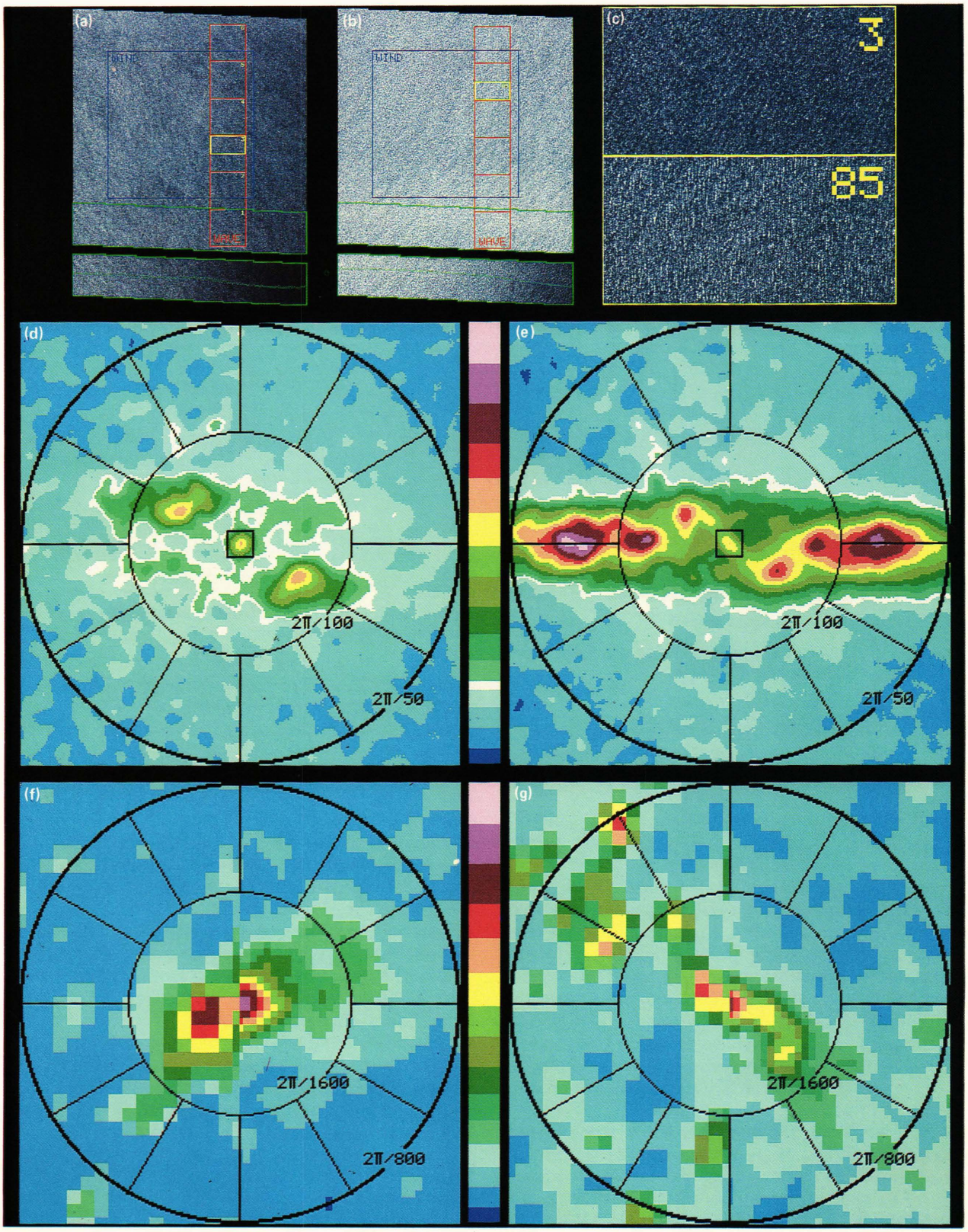

Figure 6—Two typical sets of high and low wind SAR images, with their associated wind and wave spectra, each with large and small spatial samples.

6e are shown greatly enlarged in Figs. 6f and 6g, respectively. In these figures, the outer circles correspond to wavelengths of 800 meters. Again, the left halves of the spectra are derived from 6 km samples, but the right halves are derived from 25 km image samples (the region depicted with blue borders in Figs. 6a

and 6b). In either case, however, as Fig. 5 illustrates, the local wind vector is approximately normal to the principal moment of the wind spectrum. Whether these conclusions remain valid over a broader range of environments remains to be seen.

By extracting the peak wavenumber and angle from each of the spectral estimates along the entire pass, we can estimate (in the absence of unknown intervening currents) the origin of the waves, in both time and position. Figure 7, for example, shows how the dominant wavenumber of the primary wave system evolves along the pass. The evolution can be partitioned into three separate regions, each of which can be clearly identified on Fig. 7. First, in the southernmost 600 km, we see a monotonic evolution toward smaller wavenumbers (longer wavelengths), exemplifying a linear dispersion of the waves in deep water. The longer waves, having larger group velocities, have traveled farther from the storm center. Therefore we can conclude that the satellite is also moving *away* from the storm center as it travels north. Second, abrupt changes in wavelength occur at both boundaries of the Gulf Stream, indicating strong current refraction. Third, north of the Gulf Stream, as the primary wave system enters shallow water, the local bathymetry is reflected in wavelength changes over spatial scales of just a few kilometers. As Fig. 8 shows, these shallow water wavelength changes are very sensitive indicators of the local mounds and depressions, in this case occurring in depths of at least 30 meters.

SOME REMAINING QUESTIONS

In spite of the impressive evidence that SAR is measuring real changes in the spatially evolving directional wave spectra, a number of major questions remain before SAR can be seriously advocated for an operational mission. Probably the most fundamental, and certainly the most controversial, is the problem of Doppler smear. Since SAR relies on the Doppler principle to establish position and to synthesize high resolution in the azimuth (along-track) direction, any movement of the object (i.e., contamination of the Doppler record) degrades the resulting synthesized image. For example, it can easily be shown that a radial velocity v_r of an ocean scatterer at a range R from the satellite platform traveling with velocity V will produce a position error Δx, given by

$$\Delta x = \left(\frac{R}{V}\right) v_r \ .$$

With the Seasat parameters, $R \approx 8.5 \times 10^5$ meters and $V \approx 6.6 \times 10^3$ m/sec, resulting in $R/V = 130$ seconds. A scatterer radial velocity of 1 m/sec, therefore, will produce an azimuth position shift of 130 meters. Unfortunately, the scatterers upon which we depend for ocean wave imaging are the small 30 cm waves that are riding on (or advected by) the long waves. The advection velocity (which is neither the phase nor group velocity, but is the orbital velocity of the long waves) is typically about 1 m/sec, but over a typical image sample size of several kilometers it is well characterized by a normal distribution with zero mean and a width dependent on the local sea state. The resulting Doppler smear acts like a spatial filter in the SAR directional spectra that tends to obliterate waves traveling along the direction of the spacecraft. This effect can be seen quite clearly in nearly all of the wave spectra illustrated in Figs. 3 and 6. Even at low sea states of approximately 1 meter, Seasat azimuth resolution is degraded (from 50 meters wavelength) by more than a factor of two. It is for this reason that the wave spectra of Fig. 3 can be displayed in a rectangular rather than a square format. Azimuth-traveling waves shorter than 100 meters have never been observed in Seasat imagery, even at low sea states.

THE HURRICANE IVA DILEMMA

A major hurricane can generate an extremely complex and little understood directional wave spectrum. Even for an idealized, radially symmetric and static system with known winds, wave modelers have major disagreements over the predicted wave field. In the more practical situation, when the hurricane is both

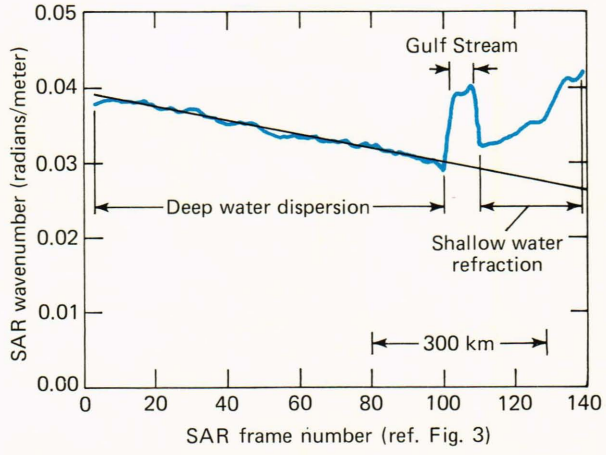

Figure 7—Spatial evolution of the dominant wavenumber along pass 1339.

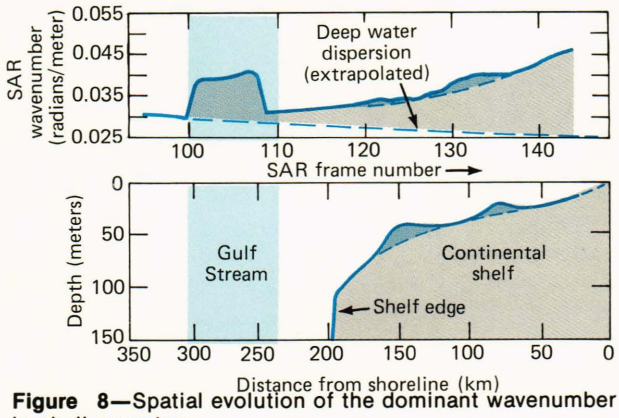

Figure 8—Spatial evolution of the dominant wavenumber in shallow water.

asymmetric and moving (often erratically), the directional wave forecast problem becomes practically intractable. This is largely because we do not yet understand the generation, propagation, and dissipation of waves in a turning and sometimes adverse wind field. Furthermore, very little data exist on the spatial and temporal evolution of the directional spectrum within hurricanes, and it is therefore not possible to clearly discriminate among the many available wave models. On the other hand, if SAR (or any other technique) could capture an instantaneous estimate of the total wave field, our understanding of the storm physics should increase dramatically.

Contained within the Seasat SAR data set is one single direct hit over the eye of a hurricane. Hurricane Iva was captured by Seasat at 0345 GMT, August 13, 1978. The importance of the data was realized early by Gonzalez et al.[14] who, in 1979, reported a thorough analysis of the storm using lower quality optically processed SAR data. Because of the uniqueness of a direct hurricane hit with an orbiting SAR, we intend next year to repeat the Gonzalez analysis of Iva at APL, but using a fully geometrically corrected and high resolution digital data set of the same quality as our pass 1339.

Iva was a minimal hurricane during the second week of August, located about 700 km southwest of Baja California and moving to the west at about 5 m/sec. Maximum sustained winds were estimated by Gonzalez et al. at 25 to 35 m/sec. By the time of the Seasat overpass, these winds had produced storm waves about 170 meters long, with a maximum height of about 6 meters.

Figure 9 is a composite of the 100-km-wide SAR image over the eye of Iva, with the wind stream lines estimated from the Seasat scatterometer in combination with GOES imagery. Iva is traveling at 5 m/sec toward the top of the figure.

A spatial matrix of 45 associated SAR directional wave spectra is superimposed on the imagery with adjacent spacings of 20 km. The satellite viewing angle is from the bottom of the figure and, because they are radially symmetric, only the top (far range) halves are displayed. As before, the outer circles of the spectra correspond to a 50 meter wavelength; the spectral origins are at their bottom centers.

Immediately apparent in all the spectra is the one dominant 170 meter wave system traveling toward the top of the figure, which is also the direction of travel of the storm. Note the systematic angular evolution of the wave system from the extreme left to the extreme right of the figure. Note also a conspicuous absence of any wave energy even close to the direction of the local wind, a condition at variance with all hurricane wave models. Doppler smearing along the direction of spacecraft travel is clearly very severe in these extremely high sea states.

Thus, Iva's spectral set may represent the clearest evidence yet for the obliteration of major wave systems from Doppler smearing. This dilemma of the missing waves in Iva will be the subject of considerable debate in the coming months as we analyze the evidence more intensively.

The only effective means of reducing the Doppler smear is through the satellite range-to-velocity ratio, R/V, or more precisely, only through R, since V is reasonably constant for all practical Rs. The effect of reducing R as a function of significant wave height H_s (where, for well-developed seas, it can be shown that $v_r \approx H_s^{1/2}$ in meter-kilogram-second units) is shown in Fig. 10. Apparently a low-altitude orbiting SAR platform is necessary to reduce azimuth smear to acceptable levels.

THE SIR-B EXPERIMENT IN THE SOUTHERN OCEAN

Fortunately, we have at least two and perhaps three orbiting SAR experiments occurring during the last half of this decade, each of which will shed further light on the value of SAR for directional ocean wave spectra.

The first of these, SIR-B (the second Shuttle Imaging Radar experiment), has already occurred and the analysis is now commencing. SIR-B, as mentioned above, was only a limited (8 day) mission, but its extremely low (230 km) altitude will allow a definitive check on the ideas presented in the previous section. SIR-B contained a Seasat-class SAR (L band, 30 meter resolution) but was capable of a variety of incidence angles. Most importantly for oceanography, the orbit had a high inclination (57°) and a very wide bandwidth digital tape recorder, rendering most of the Southern Hemisphere accessible during its early spring, when high sea states were virtually certain.

Nearly 50 separate experiments covering a number of scientific disciplines were conducted during the 8-day mission. Of those, only a few were wind-wave experiments. The most comprehensive of these occurred in the Southern Hemisphere (Fig. 11).

Conceived and coordinated by APL, the experiment was divided into two major portions:

1. A "verification" portion, consisting of a series of coincident aircraft underflight measurements, in the region around the southern tip of South America, where sea states exceeding 5 meters are common,
2. A "scientific" portion spanning a vast region of the South Atlantic but focused on a much smaller region off the southeast coast of South Africa, in the vicinity of the strong Agulhas Current.

Both portions involve some of the most interesting and dangerous areas for waves on the entire globe.

The verification portion of the experiment will involve comparing spatially evolving spectra measured by SIR-B with simultaneous and nearly coincident measurements that were taken with both an aircraft-mounted raster-scanning altimeter (the NASA "surface contour radar") and an aircraft-mounted conically scanning altimeter (the NASA "surface wave spectrometer"). During the 5 days of data collection from October 7-11, 1984, each of the three instruments

(one spacecraft and two aircraft) provided several thousand kilometers of spectral estimates over a variety of sea states and SAR incidence angles. The data should permit the most comprehensive cross comparison of spacecraft- and aircraft-measured directional spectra that has yet been conducted.

In the complementary scientific portion of the experiment, we will be attempting to track ocean swell systems in the extreme South Atlantic from their primary wind generation sources northward through the strong Agulhas Current that flows southwestward along the continental shelf of South Africa. This region of the world, particularly along the coast of Africa, is notorious for the production of extreme waves exceeding 20 meters, the result of long swells running head-on into the opposing current. With data from SIR-B, complemented with coordinated South African coastal wave measurements and profiles from the Agulhas Current, we hope to identify, track, and successfully hindcast (i.e., forecast after the fact) the spectral and spatial distribution of ocean wave energy all the way from its generation region, as it propagates through the vast Southern Ocean, and, finally, as it encounters the Agulhas Current. A quantitative comparison with conventional wave forecasting methods should clearly reveal the potential of SAR for global wave forecasting and may also shed light on the production mechanism for the extreme waves along the North Wall of the Agulhas.

Beyond SIR-B, there are at least two future possibilities for the collection of SAR ocean spectra from space. The first, a proposed but not yet approved program, is SIR-C, a NASA follow-on to SIR-B but with multiple frequency (both C and L bands) and polarization options, a near-polar orbit, and the flexible geometry and high-quality digital data of SIR-B. Like SIR-B, its successor would also be a short mission of only several days.

The next Seasat-like SAR mission appears to be ERS-1, a European Remote Sensing Satellite planned to be launched by the European Space Agency around the end of the decade. ERS-1 will orbit at 785 km in a near-polar orbit, will collect global spectra from a C-band SAR, and may feature fast turnaround (3 hours or less) data processing and dissemination. Moreover, at the 785 km altitude, even though it will probably suffer from the same Doppler smear problems as did Seasat, it should collect global ocean wave spectra over the changing seasons in both hemispheres for the first time. Table 1 summarizes the major features of a decade of spaceborne SAR wave spectra opportunities.

Table 1 — Spaceborne SAR systems for ocean wave spectra.

	Seasat	*SIR-B*	*SIR-C*	*ERS-1*
Agency	NASA	NASA	NASA	ESA
Year	1978	1984	1987	1988
Altitude (km)	800	230	200-250	785
Inclination (degrees)	72	57	Near polar	98
Swath width (km)	100	30-50	35-120	5-10
Incidence angle (degrees)	23	15-50	15-50	23
Transmitter	L band	L band	L/C bands	C band
Resolution (meters)	25	15-30	15-30	30

SPECTRASAT: A POSSIBLE LONG-TERM SOLUTION

As our Seasat analysis suggests, and as analysis on SIR-B data during 1985 and 1986 will either confirm or reject, the highest quality SAR wave spectra may come from the low-altitude missions. The higher altitude missions, generally driven by other considerations than the quality of SAR spectra (e.g., swath width, geodesy, or long lifetime), appear to suffer from intolerably excessive Doppler smear. In future SAR systems (as yet unplanned), the only practical way of reducing the Doppler smear will be to reduce the altitude of free-flying SAR satellites to that of the Shuttle, that is, to an altitude of between 200 and 250 km. Such a low altitude should be feasible through the use of active drag compensation. For example, preliminary calculations indicate that for a 230 km altitude and a 1 square meter frontal cross section, between 100 and 200 kilograms of propulsion capacity per year should be adequate.

Data rates from spaceborne SAR can be many hundreds of megabits per second, particularly if wide swaths and high resolution are desired. Consequently, construction of a synthetic aperture in real time, on board the satellite, has been frustrated by both the overwhelming data rates and the required size of the processing and storage arrays. Yet, for both wind and wave spectra, especially in deep water, the actual information rate is trivial—perhaps a kilobit per second. Moreover, there is now good evidence that reliable wind and wave spectra can be generated with spatial samples of less than 10 km. One might therefore envision a SAR system sampling the global wave field very much as the Seasat scatterometer sampled the global wind field, that is, with 500 km equatorial spacings between tracks and repetitive coverage every 3 days. Although such coverage is less than ideal for detailed storm tracking, it is at least consistent with the scatterometer coverage and is probably the best that can be expected with a single satellite.

The primary rationale for orbiting a narrow-swath SAR would be to collect global wave spectra. By themselves, these spectra would be of little value, but as a supplement and periodic update to a global wind-wave forecast model, the impact of actual mea-

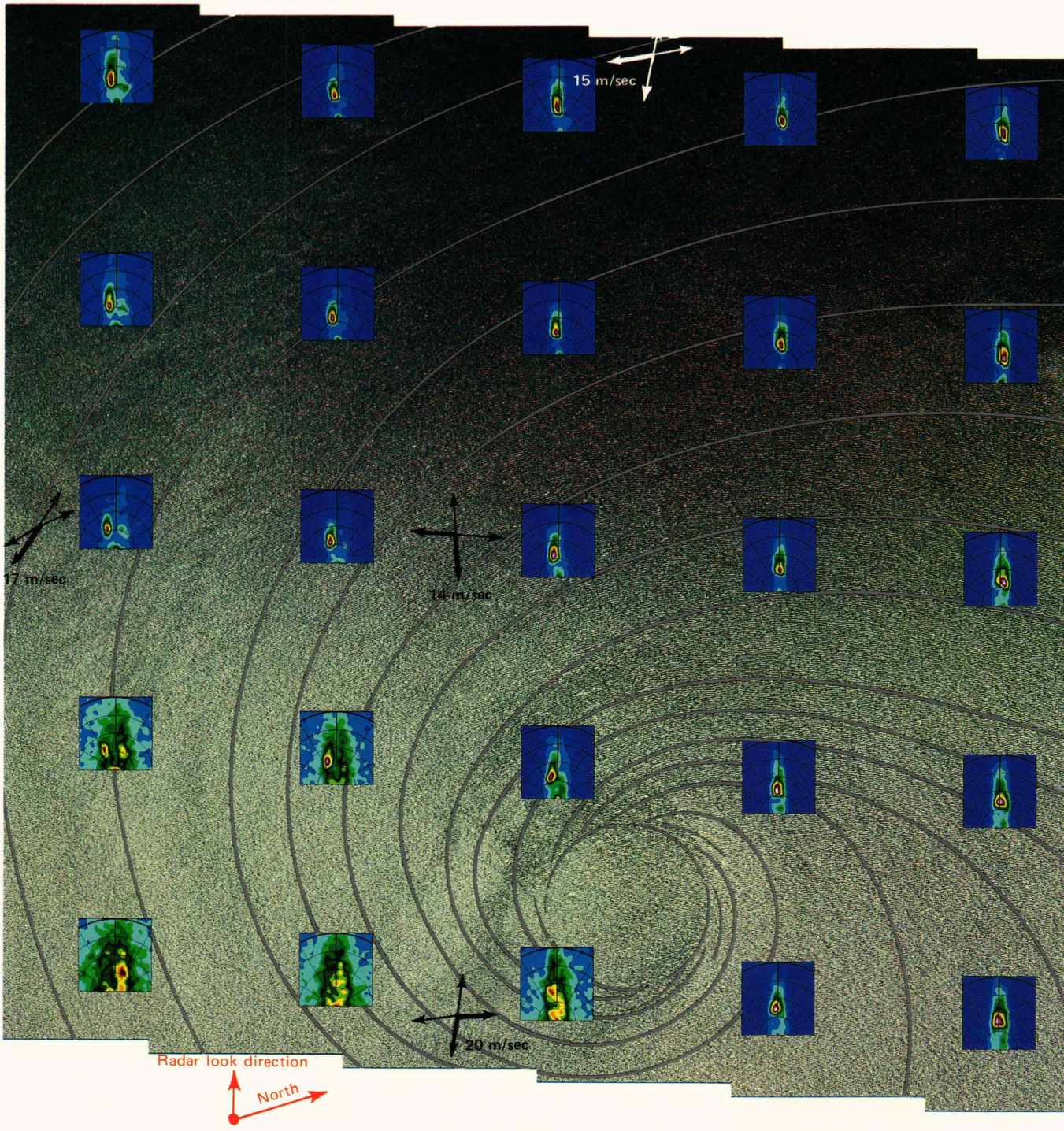

Figure 9—Hurricane Iva, showing a 100 × 175 km portion around the eye, with associated ocean wave spectra out to 50-meter wavelengths. Also shown are estimated wind stream lines and associated scatterometer wind vectors. Iva was moving toward the west at 5 m/sec. Gonzalez[14] estimates the scatterometer wind value to be low by as much as 10 m/sec.

surements of directional spectra could be revolutionary. For example, present wave-generation models in operation around the world are in gross disagreement with respect to the directional properties of waves generated from even the simplest wind fields.[15] There are no good data on the large-scale directional evolution of wind-driven waves and therefore no valid criteria for the acceptance or rejection of particular models.

The dilemma could be solved if there existed a comprehensive set of evolving winds, together with their resultant evolving (directional) waves. The SAR, although capable of precisely tracking the magnitude

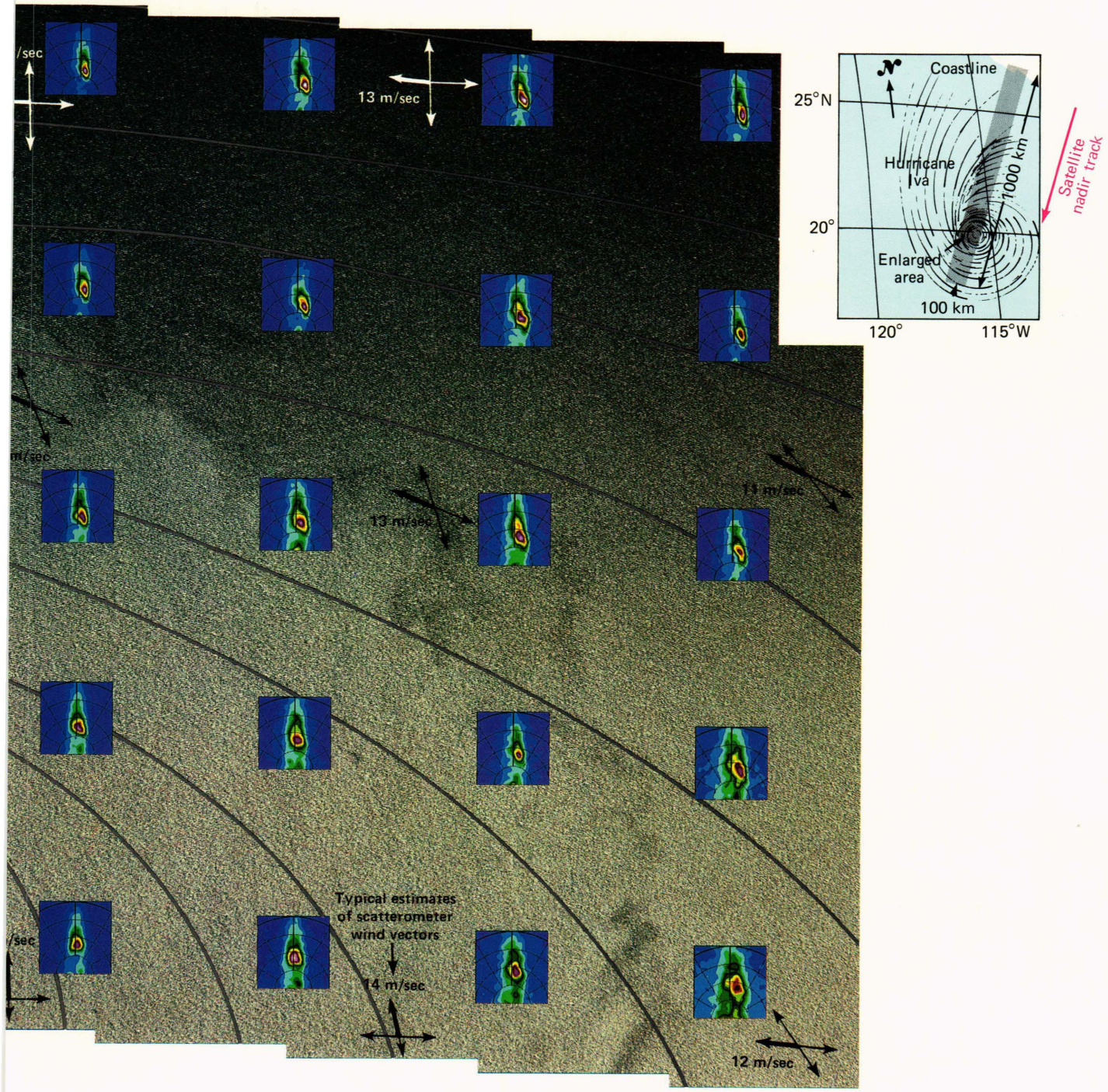

and direction of the dominant wavenumber, has generally proven elusive with respect to an estimate of the total wave energy. The problem is aggravated both by the Doppler smear effect present in existing data and by the absence of accurate and comprehensive independent estimates of wave energy. Concurrent altimeter estimates of significant wave height will probably be of value in calibrating the SAR relative directional spectra in an operational configuration.

Spectrasat[16,17] is an attempt to define the major properties of a SAR satellite specifically designed for the global collection of ocean wave spectra. Although

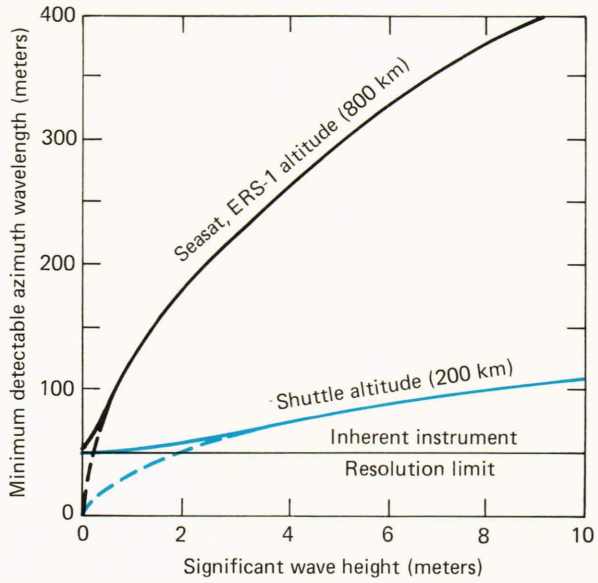

Figure 10—Advantage of a low range-to-velocity ratio, particularly in high sea states.

the initial version of Spectrasat can be quite explicit, many of the design parameters are tentative, pending an analysis of SIR-B results in 1985 and 1986. Nevertheless, it is important even now to define a "strawman" version of Spectrasat, both to stimulate debate and to aid in the design and analysis of future SAR ocean experiments.

Spectrasat (see Fig. 12) should be a low-altitude (200 to 250 km) satellite with active drag compensation. The instantaneous ground swath need be sufficient only for a statistically reliable transform, probably about 10 km or less. The small swath will allow a greatly reduced (with respect to Seasat) along-track antenna dimension, probably only 1 to 2 meters. The potentially overwhelming data rate problem is consequently alleviated, not only by the reduction in swath, but also possibly by sparse sampling of the spectra; this is similar to the scheme planned for the ERS-1 in its sampled wave mode. Global sampling strategies will depend mainly on the scale size of storms in the open ocean and on whether oceanographic significance can be attached to the observed fine-scale (less than 50 km) evolution of the dominant wave vector.

An adaptive sampling strategy, built around an onboard buffer storage and electronically steerable antenna beams, could allow increased sampling in the vicinity of developing storms and a commensurate decrease in the more benign regions. Spectrasat, or an experimental precursor, should operate in the presence of the Navy Remote Ocean Satellite System (NROSS), the ERS-1, or a similar global wind measuring system so that its directional wave spectra may be interpreted in the context of a simultaneously developing global wave forecast model. Indeed, the ultimate test of Spectrasat will be to improve significantly the wave forecast model through the addition of actual directional wave measurements.

CONCLUSIONS

Environmental monitoring of the wind and waves on global scales over both the short and long term is one of the more promising applications of radar sensors on spacecraft. Accurate measurement of directional ocean wave spectra is important not only to understand the physics of storms, but also to aid operational forecasts and to begin to accumulate a global wave climatology.

Spaceborne SAR, in the perspective of several years of intensive research, has a surprising ability to precisely monitor spatially evolving wind and wave fields over the entire globe. However, being inherently a Doppler-measuring device, the SAR smears or filters waves moving in the direction of the spacecraft. Although particularly evident in the Seasat data, there is good reason to expect nearly a factor of four improvement with the recent SIR-B experiment at its lower altitude. Additional opportunities to perform well-controlled ocean experiments will occur later in this decade, with the planned SIR-C (1987) and ERS-1 (1988) missions, each of which should substantially improve our understanding of both the measurement and the utility of global directional wave spectra.

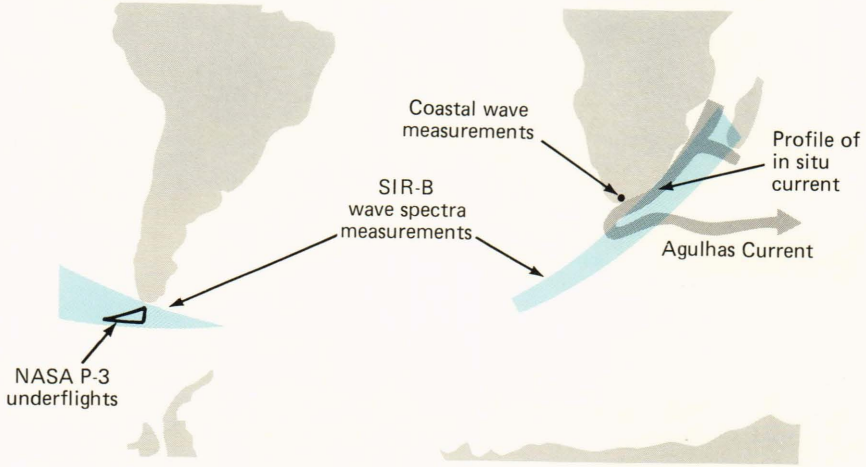

Figure 11—The SIR-B Extreme Waves Experiment in the Southern Ocean off the coasts of Chile and South Africa.

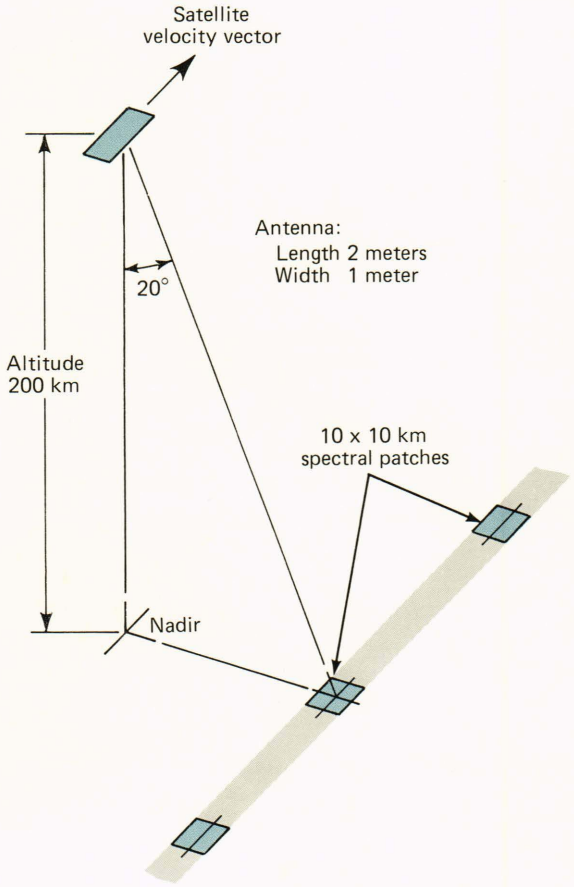

Figure 12—System geometry of Spectrasat.

REFERENCES and NOTE

[1]Encountered by the USS *Ramapo* in the Pacific Ocean on the morning of February 7, 1933.

[2]G. Mattingly, *The Armada,* especially Chap. 31, "The Long Road Home," pp. 364-375, Riverside Press, Boston (1959).
[3]C. R. Calhoun, *Typhoon: The Other Enemy,* Naval Institute Press, Annapolis (1981).
[4]W. Bascom, *Waves and Beaches,* Anchor Books, Garden City, N.Y., pp. 152-161 (1980).
[5]H. Jeffries, "On the Formation of Waves by Wind," in *Proc. R. Soc. London* **A110,** pp. 341-347 (1924).
[6]F. Ursell, "Wave Generation by Wind," in *Surveys in Mechanics,* (G. K. Batchelor, ed.), Cambridge University Press, pp. 216-249, (1956).
[7]W. J. Pierson, Jr., G. Neumann, and R. W. James, *Practical Methods for Observing and Forecasting Ocean Waves by Means of Wave Spectra and Statistics,* U.S. Navy Hydrographic Office Publication No. 603 (reprinted 1960) (1955).
[8]F. S. Ellers, "Advanced Offshore Oil Platforms," *Sci. Am.* **246,** 39-49 (1982).
[9]G. C. Ewing (ed.), *Oceanography from Space,* Woods Hole Oceanographic Institution Report NASA-CR-64164 (1965).
[10]R. C. Beal, P. S. DeLeonibus, and I. Katz (eds.), *Spaceborne Synthetic Aperture Radar for Oceanography,* The Johns Hopkins University Press, Baltimore (1981).
[11]L. L. Fu and B. Holt, *Seasat Views Oceans and Sea Ice with Synthetic Aperture Radar,* Jet Propulsion Laboratory Pub. 81-120 (1982).
[12]A. H. Woodcock, "Soaring Over the Open Sea," *Sci. Mon.* **55,** 226-232 (1942).
[13]T. W. Gerling, *Fine Scale Structure of the Wind Field from Seasat SAR Imagery* (in preparation, 1984).
[14]F. I. Gonzalez, T. W. Thompson, W. E. Brown, Jr., and D. E. Weissman, "Seasat Wind and Wave Observations of Northeast Pacific Hurricane IVA, August 13, 1978," *J. Geophys. Res.* **87,** 3431-3438 (1982).
[15]O. M. Phillips and K. Hasselmann (eds.), *The Sea Wave Modelling Project* (*SWAMP*), Plenum Press, New York (in press).
[16]R. C. Beal, *Spectrasat:* "A Concept for the Collection of Global Directional Wave Spectra," in *Proc. 1984 International Geoscience and Remote Sensing Symp.,* Strasbourg, Aug 27-30, 1984.
[17]R. C. Beal and R. L. Jordan, "Global Wave Spectra from SAR: System Design Considerations," in *Oceans '84 Conf. Record,* Washington, D.C. (1984).

ACKNOWLEDGMENTS—I thank D. G. Tilley for the computation and display of SAR wave spectra (Figs. 3, 6, and 9), as well as the cover of this issue, T. W. Gerling for the analysis of the scatterometer and SAR wind spectra (Figs. 2, 3, 4, and 5), and F. M. Monaldo for the analysis of the evolving SAR wave spectra (Figs. 7 and 8). This work was sponsored jointly by NASA, the Office of Naval Research, and internal research and development funds.